Geological Survey of Japan Cruise Report No. 21, p. 231-249, 1986

XV. LOCAL VARIABILITY OF MANGANESE NODULE CHEMISTRY AROUND THE SMALL ABYSSAL HILLS IN THE GH81-4 AREA

Akira Usui and Shigeru Terashima

Introduction

Earlier numerous chemical analyses have revealed significant variations in nodule chemistry on various scales; high-grade nodule provinces in the Northeastern Equatorial Pacific (HEIN, 1977; PIPER and LEONG, 1979), local great variation around topographic highs (HALBACH and ÖZKARA, 1979). The small-scale compositional variations of manganese nodules have been one of economic and scientific interests. However, the pattern of local variation in nodule chemistry, morphology, mineralogy, and their relationships to topography and geology have not been well understood. In the GH81-4 area, small-scale nodule sampling were made in the two model sites (40×40 km^2), Areas I and II, after bathymetric and geophysical surveys.

This article aims at describing the mode of local variation of nodule chemistry and its relationships to nodule mineralogy, and external and internal structure.

Samples

One hundred and eight nodule samples were prepared from every station where nodules were collected. Each sample from a station includes several entire nodules so that the sample represents approximate mean bulk compositions of the stations. Morphological description of nodule samples and semiquantitative X-ray diffraction analyses on the powder samples were performed before chemical analysis. Analysis numbers are common to those for X-ray diffraction analysis in Table XV-1 (USUI, this cruise report).

Analytical methods

Air-dried nodule samples were ground in an agate mortar into powder under 100 mesh. The untreated powder samples are divided into two to be subjected to element chemical analyses and gravimetric analysis of water contents. Mn, Fe, Cu, Ni, Co, Pb, Zn, Si, Al, and water contents were determined according to the method of GSJ (Geological Survey of Japan) standard (TERASHIMA, 1978; MOCHIZUKI and TERASHIMA, 1983). The powder is melt with sodium carbonate and boric acid, and the fusion was dissolved with dilute (1:9) hydrochloric acid. Lanthanum chloride was added to the solution to prevent interference of other components. Element concentrations were determined by atomic absorption spectroscopy. Water contents were determined as H_2O^+ and H_2O^-, by Penfield Method and by drying in ovens at 110°C for three hours, respectively.

All data of chemical and mineral analyses are recorded as data files and processed using a personal computer system.

Table XV-1 Chemical composition of manganese nodules in the GH81-4 area.

No.	Station	Sample	Type	Mineral abundance T	Mineral abundance D	Chemical composition (in wt. %) Mn	Fe	Cu	Ni	Co	Pb	Zn	Si	Al	H_2O^+	H_2O^-	Area	Remarks
1	2577	FG313	R2	xxx	+	31.62	5.51	1.92	1.89	0.10	0.021	0.152	5.12	1.98	10.24	15.94	I	one nodule
2	2578	FG314	R2	xxx	+	28.10	5.53	1.65	1.74	0.09	0.032	0.141	7.00	2.70	11.74	14.25	I	one nodule
3	2579	P218	-	xxx	+	48.06	0.31	0.14	0.48	0.00	0.008	0.058	1.95	0.41	10.29	6.50	I	pipe(32cm depth)
4		P218	-	xx	xx	43.72	0.49	0.14	1.10	0.00	0.002	0.066	3.20	0.72	10.00	8.44	I	cusps(32cm depth)
5		P218	-	xxx	x	45.63	0.56	0.31	0.32	0.00	0.007	0.021	4.21	0.91	9.51	5.01	I	plate(32cm depth)
6		FG315	R2	xxx	+	28.22	5.50	1.57	1.95	0.10	0.031	0.131	7.12	2.68	3.80	15.81	I	2 nods.
7	2580	FG322-1	I2	xx	+	25.83	11.21	1.15	1.20	0.20	0.054	0.103	5.32	2.19	11.64	22.37	-	one nodule
8		-2	I2	xx	x	25.61	11.46	1.12	1.09	0.21	0.063	0.101	5.63	2.18	11.67	20.31	-	one nodule
9	2581	FG311	R2	xxx	+	26.20	7.62	1.41	1.52	0.14	0.033	0.113	7.30	2.71	12.00	17.04	-	one nodule
10	2582	FG312	R2	xxx	+	31.70	5.48	1.93	1.77	0.11	0.022	0.164	4.85	1.91	10.37	16.73	I	2 nods.
11	2583	P220	R2	xx	x	17.21	7.53	0.88	1.18	0.08	0.035	0.079	13.28	4.98	nd	14.97	I	one nodule(core top)
12		FG327	R2	xxx	+	30.72	5.92	1.85	1.60	0.11	0.021	0.150	5.12	1.84	9.90	20.28	I	4 nods.
13	2588	FG317	R2	xxx	+	33.50	4.78	2.06	1.71	0.10	0.030	0.178	4.41	1.68	10.27	15.66	I	half a nodule
14	2594	FG316-1	R2	xxx	+	31.42	5.46	1.81	1.85	0.10	0.034	0.144	4.95	1.72	10.33	17.06	-	2 nods.
15		-2	R1	xx	x	26.31	10.47	1.16	1.28	0.19	0.052	0.099	5.60	1.98	11.63	20.49	-	2 nods.
16	2596	FG342	R2	xxx	+	31.82	5.38	1.95	1.93	0.12	0.028	0.161	4.58	1.87	10.41	16.57	-	2 nods.
17	2597	FG341-1	R2	xxx	+	32.15	5.12	1.90	1.96	0.11	0.025	0.149	4.50	1.96	10.47	16.91	-	3 nods.
18		-2	R2	xxx	+	32.10	5.49	1.87	1.90	0.10	0.031	0.152	4.71	1.88	10.55	16.89	-	one nodule
19	2598	FG329	R2	xxx	+	31.92	6.00	1.84	1.74	0.13	0.021	0.150	5.06	1.90	10.44	17.29	-	2 nods.
20	2605	FG335	R1	xx	x	26.00	10.52	1.24	1.28	0.19	0.042	0.102	5.61	2.22	11.45	21.35	II	one nodule
21	2606	FG334	R2	xxx	+	32.96	5.21	1.93	1.87	0.10	0.016	0.180	4.25	1.71	10.50	17.11	II	3 nods.
22	2608	FG338	R2	xxx	+	30.75	5.80	1.82	1.74	0.12	0.025	0.135	5.29	2.05	10.78	17.84	II	3 nods.
23	2609	FG343	R2	xxx	+	31.50	5.35	1.88	1.86	0.11	0.025	0.156	5.00	1.87	10.34	17.54	I	2 nods.
24	2610	FG344	R2	xxx	+	32.61	5.34	1.90	1.79	0.10	0.020	0.168	4.22	1.71	10.48	16.18	I	2 nods.
25	2611	FG345	R2	xxx	+	29.80	5.75	1.77	1.85	0.11	0.028	0.154	5.81	2.06	11.34	16.36	I	one nodule
26	2617	FG350	I1	xx	x	25.52	11.80	1.02	1.20	0.25	0.068	0.096	5.20	1.92	12.71	18.49	I	one nodule
27	2619	FG351	R2	xxx	+	31.28	5.88	1.84	1.90	0.11	0.022	0.156	5.35	1.95	9.65	17.45	I	3 nods.
28	2620	FG352	R2	xxx	+	29.60	6.63	1.76	1.81	0.14	0.027	0.133	5.88	2.21	10.54	18.79	I	3 nods.
29	2621	FG353	S1	x	xx	23.02	12.30	0.85	0.95	0.21	0.062	0.082	6.20	2.37	11.56	22.18	I	2 nods.
30	2622	B59	S1	x	xx	25.21	12.56	1.06	0.91	0.22	0.059	0.094	5.11	1.86	11.86	22.49	I	2 nods.(core top)
31	2624	FG355	R2	xxx	+	30.22	6.70	1.94	1.62	0.16	0.038	0.139	5.00	2.09	10.58	20.83	I	3 nods.
32	2625	FG356	R2	xxx	+	29.71	7.21	1.83	1.54	0.17	0.022	0.134	5.10	2.08	10.73	20.46	I	3 nods.
33	2626	FG357	R2	xxx	+	29.90	6.82	1.73	1.69	0.15	0.024	0.133	5.53	2.09	9.13	18.69	I	4 nods.
34	2627	FG358	R2	xxx	+	30.02	6.45	1.80	1.75	0.15	0.023	0.140	5.31	2.00	10.46	20.60	I	2 nods.
35	2628	B60	R2	xxx	+	30.05	6.45	1.79	1.67	0.16	0.023	0.133	5.00	2.10	11.10	17.66	I	2 nods.(core top)
36			R2	xxx	+	30.00	6.34	1.72	1.70	0.15	0.025	0.138	4.67	1.94	10.69	18.26	I	2 nods.(core top)
37	2630	FG360	R2	xxx	+	32.03	5.55	1.68	1.71	0.10	0.024	0.157	4.70	1.76	10.07	18.03	I	2 nods.
38	2631	FG361	R2	xxx	+	33.95	5.07	1.80	1.84	0.10	0.023	0.164	4.65	1.74	10.68	16.82	I	2 nods.
39	2632	FG362	S1	x	xx	24.81	12.40	0.89	0.94	0.21	0.059	0.087	5.81	2.00	11.30	23.13	I	2 nods.

Table XV-1 (continued)

No.	Station	Sample	Type	Mineral abundance T	Mineral abundance D	Chemical composition (in wt. %) Mn	Fe	Cu	Ni	Co	Pb	Zn	Si	Al	H_2O^+	H_2O^-	Area	Remarks
40	2633	FG363	S1	+	xx	18.19	13.70	0.45	0.50	0.19	0.070	0.063	9.24	3.36	10.89	22.50	I	2 nods.
41	2634	B61	S1	x	xx	15.38	13.32	0.44	0.58	0.15	0.048	0.061	11.05	4.12	10.72	19.98	I	2 nods.
42	2635	FG364	S1	x	x	23.30	11.21	0.89	1.00	0.21	0.063	0.085	7.14	2.75	10.85	22.90	I	2 nods.
43	2636	FG365	R2	xxx	+	33.18	5.40	1.80	1.71	0.12	0.024	0.150	5.20	1.68	10.13	18.14	I	2 nods.
44	2637	FG366	R2	xxx	+	32.20	5.40	1.78	1.78	0.12	0.038	0.153	5.55	1.74	10.17	17.75	I	4 nods.
45	2638	FG367	R2	xxx	+	30.48	5.44	1.80	1.67	0.12	0.029	0.146	5.53	1.74	10.53	18.45	I	3 nods.
46	2640	FG368	S2	xx	+	24.15	10.51	1.12	1.02	0.19	0.043	0.094	6.92	2.10	11.30	19.85	I	2 nods.
47			R2	xxx	+	31.13	5.27	1.88	1.66	0.13	0.024	0.162	5.02	1.85	9.78	20.51	I	half/ 4cm dia.
48			R2	xxx	+	31.11	5.45	1.85	1.68	0.12	0.035	0.159	5.27	1.88	8.92	19.85	I	2 nods./ 2.5cm dia.
49			R2	xxx	+	30.38	5.40	1.80	1.93	0.13	0.035	0.144	5.60	1.92	9.99	19.92	I	4 nods./ 1-2cm dia.
50			R2	xxx	+	30.20	4.56	1.77	2.05	0.12	0.031	0.145	6.12	2.20	9.42	20.93	I	7 nods./ 0.5cm dia.
51	2642	FG370	R2	xxx	+	30.25	5.23	1.81	1.79	0.10	0.028	0.156	5.41	1.87	9.96	16.80	I	2 nods.
52	2644	FG372	R2	xxx	+	29.55	5.03	1.86	1.80	0.11	0.035	0.151	5.75	2.00	9.85	15.48	I	2 nods.
53	2645	B63	S1	-	xx	9.27	21.20	0.52	0.32	0.26	0.067	0.050	12.98	2.08	10.91	21.24	I	2 nods.(15cm depth)
54			S1	+	xx	11.70	20.10	0.58	0.40	0.30	0.066	0.056	12.00	2.07	10.35	22.13	I	2 nods.(15cm depth)
55	2646	FG373	R1	xx	x	24.75	8.55	1.26	1.23	0.18	0.045	0.133	7.22	2.33	10.47	17.83	I	2 nods.
56	2647	FG374	R1	x	x	24.72	13.84	0.80	0.94	0.25	0.071	0.087	5.31	1.68	11.46	21.33	I	one nodule
57	2648	FG375	R2	xxx	+	30.02	7.26	1.81	1.63	0.15	0.037	0.134	5.36	2.04	10.59	20.46	I	2 nods.
58	2649	FG376	R2	xxx	+	30.00	7.26	1.94	1.58	0.17	0.031	0.136	5.40	2.04	10.17	21.10	I	2 nods.
59	2650	FG377	I1	xx	x	24.98	9.81	1.27	1.17	0.18	0.042	0.112	7.10	2.44	11.04	19.80	I	2 nods.
60	2651	P224	I2	xx	+	29.47	9.76	1.58	1.30	0.19	0.045	0.123	5.01	1.96	9.77	18.63	I	one nodule (core top)
61	2652	FG378	S1	x	xx	24.80	12.45	0.95	1.02	0.21	0.052	0.085	6.09	2.32	11.26	21.94	I	2 nods.
62	2653	FG379	S1	x	xx	18.71	13.41	0.63	0.68	0.19	0.051	0.074	9.33	3.55	10.81	19.36	I	one nodule
63	2654	FG380	S1	x	xx	23.55	15.30	0.62	0.73	0.24	0.080	0.074	5.58	1.94	11.95	23.02	I	one nodule
64	2655	FG381	I2	xxx	+	30.50	8.65	1.69	1.39	0.18	0.033	0.122	5.25	2.08	11.00	19.66	I	2 nods.
65	2656	FG382	R2	xxx	+	33.35	5.11	1.90	1.90	0.10	0.030	0.174	5.10	1.80	9.73	16.81	I	3 nods.
66	2657	B64	R2	xxx	+	32.10	5.80	1.86	1.75	0.11	0.029	0.148	5.44	1.91	10.37	16.26	I	3 nods.(core top)
67	2659	FG384	S1	+	xx	23.12	16.68	0.59	0.59	0.26	0.077	0.073	5.02	1.60	11.92	23.04	I	1/4 nodules
68	2660	FG385	I1	x	+	25.60	12.31	0.99	0.99	0.26	0.068	0.106	5.28	2.07	11.52	22.23	I	half a nodule
69	2661	FG386	I2	xxx	+	29.27	7.55	1.86	1.46	0.16	0.026	0.132	5.20	2.05	10.72	18.79	I	2 nods.
70	2662	FG387	R2	xxx	+	31.26	5.81	1.80	1.72	0.11	0.026	0.160	5.22	1.90	10.23	17.40	I	2 nods.
71	2663	P225	R2	xx	x	28.50	7.58	1.69	1.35	0.14	0.033	0.118	5.24	1.87	11.04	19.92	I	1/4 nods.(core top)
72	2666	FG390	R2	xxx	+	33.30	5.30	1.95	1.71	0.10	0.030	0.176	4.51	1.80	10.05	15.66	I	2 nods.
73	2667	FG391	R2	xxx	+	33.52	5.30	1.97	2.00	0.10	0.041	0.158	4.92	1.86	10.38	16.20	I	2 nods.
74	2668	FG392	R2	xxx	+	32.71	5.43	1.95	1.93	0.11	0.035	0.155	5.30	1.91	10.10	19.12	I	3 nods.
75	2669	B65	R2	xxx	+	32.37	5.71	1.83	1.74	0.12	0.024	0.170	5.26	1.77	10.17	15.44	I	one nodule/ 1.5cm (core top)
76			R2	xxx	+	30.83	5.67	1.77	1.96	0.11	0.029	0.146	5.68	1.98	10.43	15.76	I	3 nods./ 0.5-1cm dia. (do.)

Table XV-1 (continued)

No.	Station	Sample	Type	Mineral abundance T	Mineral abundance D	Chemical composition (in wt. %) Mn	Fe	Cu	Ni	Co	Pb	Zn	Si	Al	H_2O^+	H_2O^-	Area	Remarks
77			R2	xxx	x	28.90	5.40	1.56	1.90	0.12	0.032	0.123	7.22	2.50	9.61	16.89	I	25 nods./ 0.5cm(do.)
78	2670	FG424	R2	xxx	+	32.45	5.68	1.99	1.64	0.12	0.027	0.160	4.91	1.80	9.31	18.86	I	half a nodule
79			R2	xxx	+	32.12	5.81	1.92	1.87	0.12	0.030	0.148	5.03	1.85	9.99	18.54	I	2 nods./ 1.5cm dia.
80			R2	xxx	+	30.61	6.01	1.78	1.90	0.11	0.019	0.138	6.25	2.05	9.92	18.21	I	3 nods./ 1cm dia.
81			R2	xxx	+	27.21	5.97	1.54	1.85	0.12	0.041	0.128	8.00	2.53	9.38	18.37	I	5 nods./ 0.5cm dia.
82	2671	FG425	R2	xxx	+	29.10	5.24	1.63	1.90	0.10	0.019	0.134	7.05	2.67	10.12	16.21	I	4 nods.
83	2672	FG426	R2	xxx	+	30.11	4.49	1.74	2.05	0.11	0.023	0.127	6.04	2.35	nd	14.00	I	2 nods.
84	2677	FG394	R2	xxx	+	34.63	5.00	1.95	1.77	0.11	0.027	0.181	4.55	1.81	10.02	17.88	II	3 nods.
85	2678	FG395	R2	xxx	+	31.86	5.49	1.72	1.85	0.12	0.035	0.158	5.90	2.13	8.62	17.49	II	3 nods.
86	2679	FG396	R2	xxx	+	35.01	5.10	1.95	1.71	0.10	0.027	0.180	4.65	1.70	10.20	16.52	II	one nodule
87	2680	FG397	R2	xxx	+	34.30	5.24	1.96	1.81	0.10	0.033	0.169	4.75	1.74	10.48	16.57	II	one nodule
88	2681	B66	R2	xxx	+	33.02	5.40	1.78	1.93	0.11	0.032	0.151	5.22	1.97	10.63	17.41	II	2 nods.(core top)
89	2684	FG400	R2	xxx	+	33.43	5.00	1.80	1.97	0.10	0.030	0.129	4.91	2.13	10.42	15.69	II	3 nods.
90	2686	FG402	R2	xx	+	29.04	7.35	1.67	1.50	0.14	0.031	0.116	6.68	2.31	9.97	20.89	II	2 nods.
91	2687	FG403	R2	xx	x	27.10	8.20	1.49	1.31	0.16	0.036	0.105	6.57	2.36	10.04	21.18	II	2 nods.
92	2690	FG405	R2	xxx	+	34.12	5.10	1.70	2.06	0.11	0.036	0.130	4.48	1.87	11.24	16.14	II	2 nods.
93	2692	FG407	I1	xx	x	22.92	9.30	1.14	1.11	0.16	0.039	0.088	8.93	2.96	9.93	18.80	II	2 nods
94	2693	FG408	R2	xxx	+	32.84	5.40	1.90	1.74	0.12	0.036	0.155	5.19	1.75	9.99	17.75	II	3 nods.
95	2695	B67	R1	xx	+	19.90	8.12	1.03	1.07	0.11	0.028	0.084	12.00	3.84	8.81	15.12	II	one nodule(core top)
96	2696	FG410	R2	xxx	+	32.61	4.91	1.91	1.85	0.10	0.030	0.170	4.84	1.87	9.90	16.98	II	2 nods.
97	2698	FG412	R2	xxx	+	33.03	5.10	1.92	1.77	0.10	0.021	0.175	4.90	1.75	10.06	15.58	II	one nodule
98	2699	FG413	R2	xxx	+	33.60	4.70	1.90	1.91	0.10	0.018	0.176	4.80	1.87	11.77	15.40	II	2 nods.
99	2705	B68	R2	xx	x	27.55	7.76	1.48	1.70	0.19	0.044	0.111	6.37	2.32	nd	15.44	II	2 nods.(core top)
100	2706	FG418	R2	xxx	+	33.46	5.00	1.89	1.84	0.10	0.019	0.173	4.92	1.89	10.55	16.28	II	3 nods.
101	2710	FG422	R2	xxx	+	32.02	5.70	1.80	1.68	0.12	0.029	0.146	5.00	1.75	10.11	18.53	II	2 nods.
102	2711	FG423	I1	xx	x	23.90	9.90	1.15	1.09	0.18	0.052	0.093	7.85	2.84	10.70	19.48	II	half a nodule
103	2712	P229	R1	xx	x	26.42	10.77	1.20	1.13	0.22	0.061	0.098	5.12	2.03	11.21	20.75	II	one nodule(core top)
104	2713	D496	-	+	xx	22.94	17.20	0.40	0.54	0.28	0.074	0.058	3.78	1.16	12.42	23.68	I	crust/ 1cm thick
105			S1	xx	xx	25.50	10.75	1.14	1.11	0.22	0.051	0.092	5.75	1.89	11.90	21.56	I	one nodule
106			R2	xxx	+	31.61	5.32	2.09	1.66	0.14	0.029	0.137	4.91	1.89	10.67	20.35	I	1/4 nodules/5cm dia.
107			R2	xxx	+	31.02	5.78	1.83	1.82	0.10	0.005	0.153	5.75	2.20	9.31	17.08	I	4 nods. / 1.5cm dia.
108	2635	FG364	R2	xx	x	24.40	9.57	1.18	1.31	0.22	0.046	0.102	7.83	2.70	11.02	19.36	I	3 nods.

Nodule type/ R, I, and S denote rough, intermediate, and smooth surface nodules. R1: IDr/IDPr, R2: Sr/Dr, I1: IDs.r/IDPs.r, I2:Ss.r/Ds.r, S1:IDs/IDPs, S2: Ss/Ds.

Mineral abundance/ T:10Å manganate, D: δ-MnO_2. xxx: very abundant, xx:abundant, x: present, +:tranceable, -: none.

Chemical compositions are expressed in wt. %. All metal elements and H_2O^+ are normalized to 110°C dried samples, but H_2O^- is to air-dried samples. nd: no data.

Results and discussion

Element concentrations and water content (H_2O^+) are normalized to 110°C dried powder samples, and loss of heating at 110°C is to air-dried samples. Numerical results are listed in Table XV-1 together with nodule type and selected mineralogical data.

General compositional features

Concentrations of major metal element concentrations of manganese nodules of this area are within the range of the Pacific deep-sea nodules (HEIN, 1977). The average of nickel plus copper grade exceed 3 wt.%, which is comparable or even greater than those from the Northeastern Equatorial Manganese Nodule Belt. The nodules seem to be high-graded, though abundance is relatively low and areal distribution is limited.

When converted to oxides (MnO_2, Fe_2O_3, CuO, NiO, Co_2O_3, PbO, ZnO etc.) the analyses of nodules sum to between 81 to 94 wt.% with the average of 88 wt.%. Manganese is always a major element of these nodules ranging from 15 to 35 wt.%, whereas iron is usually lower and depleted to less than 5% in some cases. Other metal elements, Cu, Ni, Co, Pb, and Zn are apt to covary with the two major elements. Cu, Ni, and Zn are positively correlated with Mn, and Co and Pb with Fe. Si and Al may be attributable to nodule nuclei and included rock fragments and detritals.

The nodules from the GH81-4 area are characteristic of great variability in chemical composition, as most distinctly represented by Mn/Fe ratio. The ratio varies from 1.2 to 7.1 for nodules from sediment surfaces. The compositional variation of nine metal elements of these nodules are within the range of normal deep-sea manganese nodules. Some exceptionally high and low ratios are encountered in nodules buried within sediment cores: Mn/Fe=155 (P218 buried at 32 cm depth) and 0.44 (B63 buried at 15 cm depth).

Mineralogical controls of nodule chemistry

Earlier chemical and mineral investigations combined with precise morphological descriptions (USUI *et al.*, 1978; USUI, 1979) have concluded that principal mineral constituents of deep-sea manganese nodules are as follows.

1) 10 Å manganate phase: iron-free and nearly stoichiometric hydrous manganate mineral containing lattice-held Cu, Ni, and Zn. The ratio (Cu+Ni+Zn)/Mn falls on around 0.16 or less. The phase represents rough surfaces on nodules in the form of cusps or dendrites. It is deposited from dissolved metals in interstitial water of unconsolidated surface sediments in the course of early diagenesis of sediments.

2) δ-MnO_2 phase: submicroscopic mixture of poorly crystalline 2 line form δ-MnO_2 and amorphous hydrous ferric oxide, containing similar amount of Mn and Fe. Cu, Ni, and Zn concentrations are much depleted as compared with 10 Å manganate. The phase represents smooth surfaces on nodules in the form of stratified layers with occasional columnar patterns. It is deposited from overlying normal sea water as settling colloidal particles.

3) Mn-free silicate minerals and nuclei: fine particles of clay minerals, zeolites, plagioclases, quartz, etc. in oxide layers, and nuclei.

The nodule surface structures, rough and smooth, are consequently correspondent

Table XV-2 Average chemical compositions of manganese nodules.

Morphological type	Sr/Dr	Ss·r/Ds·r	IDr/IDPr	IDs·r/IDPs·r	IDs/IDPs/Ds	P218 (−32 cm)	B62 (−15 cm)	Total
(in Table XV-1)	R2	I2	R1	I1	S1+S2	—	—	
Number of analysis	74	5	6	5	13	3	2	103
Mn	30.98	28.14	24.68	24.58	20.50	45.80	10.49	29.10
	±2.60	±2.26	±2.46	±1.15	±5.42	±2.17	—	±4.10
Cu	1.79	1.48	1.12	1.11	0.74	0.20	0.55	1.50
	±0.18	±0.33	±0.17	±0.11	±0.23	±0.10	—	±0.42
Ni	1.77	1.29	1.12	1.11	0.75	0.63	0.36	1.56
	±0.17	±0.17	±0.13	±0.08	±0.26	±0.41	—	±0.39
Zn	0.147	0.116	0.101	0.099	0.075	0.048	0.053	0.123
	±0.020	±0.014	±0.017	±0.010	±0.014	±0.024	—	±0.031
Fe	5.80	9.73	10.38	10.62	14.26	0.45	20.65	7.43
	±0.93	±1.67	±2.03	±1.33	±3.24	±0.13	—	±3.00
Co	0.120	0.188	0.190	0.206	0.221	0.00	0.28	0.143
	±0.024	±0.019	±0.047	±0.046	±0.046	—	—	±0.050
Pb	0.029	0.044	0.050	0.054	0.062	0.006	0.067	0.036
	±0.007	±0.015	±0.014	±0.010	±0.010	±0.003	—	±0.015
Si	5.50	5.28	6.81	6.87	7.79	3.12	12.49	5.79
	±1.23	±0.23	±2.65	±1.63	±2.79	±1.13	—	±1.52
Al	2.04	2.09	2.35	2.45	2.45	0.68	2.08	2.12
	±0.44	±0.10	±0.76	0.46	±0.77	±0.25	—	±0.53
H_2O^+	10.18	10.96	10.84	11.18	11.25	9.93	10.63	10.47
	±0.97	±0.78	±1.07	±1.03	±0.54	±0.39	—	±1.03
H_2O^-	17.6	19.9	19.5	19.8	22.0	6.7	21.7	10.5
	+1.8	+1.5	+2.5	+1.5	+1.2	+1.7	—	+2.3
Mn/Fe	5.50	2.99	2.43	2.33	1.55	109	0.51	4.57
	±1.03	±0.73	±0.36	±0.20	±0.58	±40	—	±1.76
Cu+Ni+Zn	3.71	2.88	2.37	2.33	1.56	0.87	0.96	3.26
	±0.32	±0.49	±0.31	±0.17	±0.49	±0.37	—	±0.83

*Numerical data from Table XV-1. Standard deviation with ±. Total: data of P218 and B63 excluded.

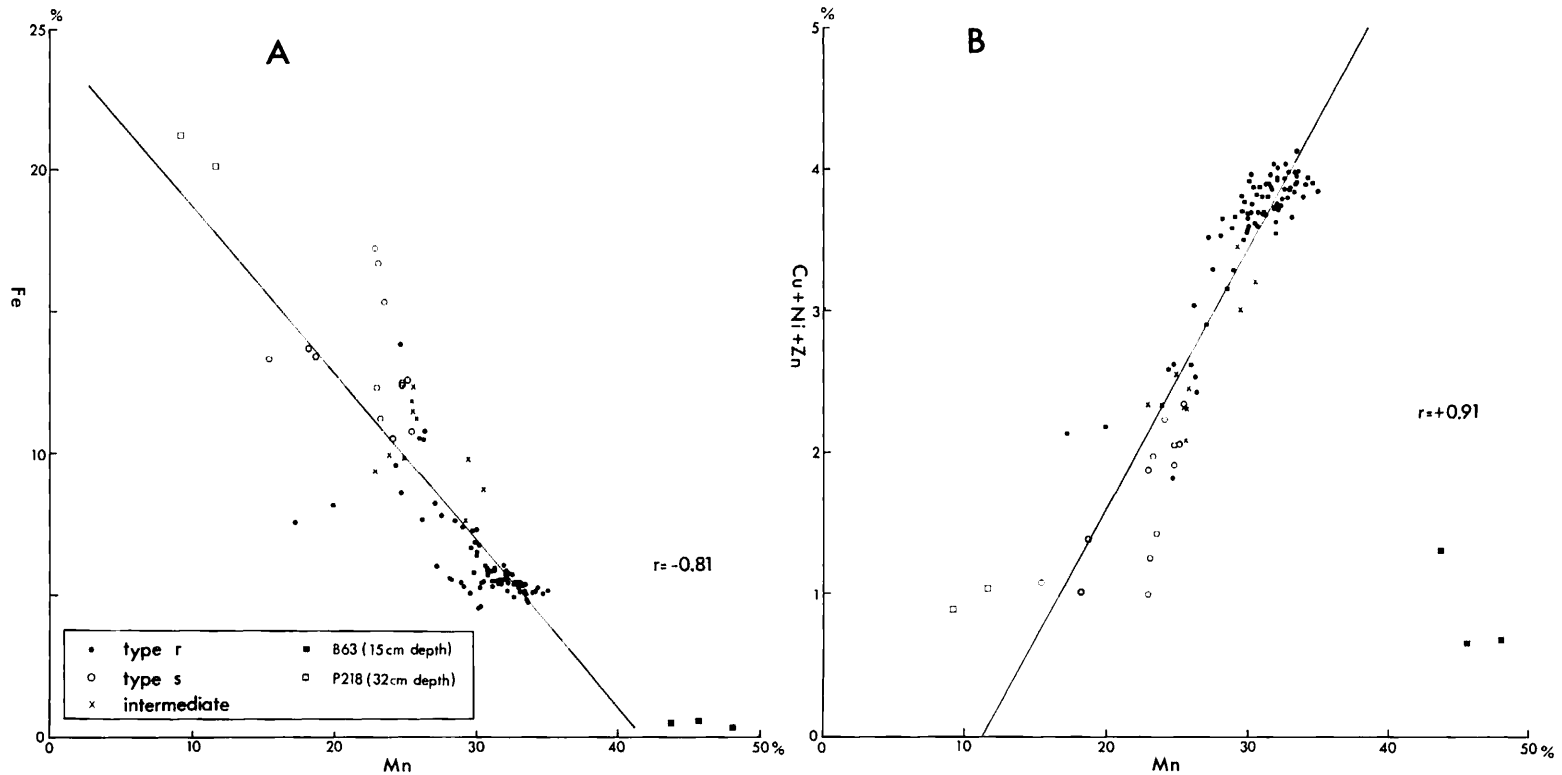

Fig. XV-1(1)

Fig. XV-1 Correlation plots of chemical and mineral compositions. Symbols for nodule morphology are common in six figures. Regression curves are based on 103 data sets except for P218 and B63.

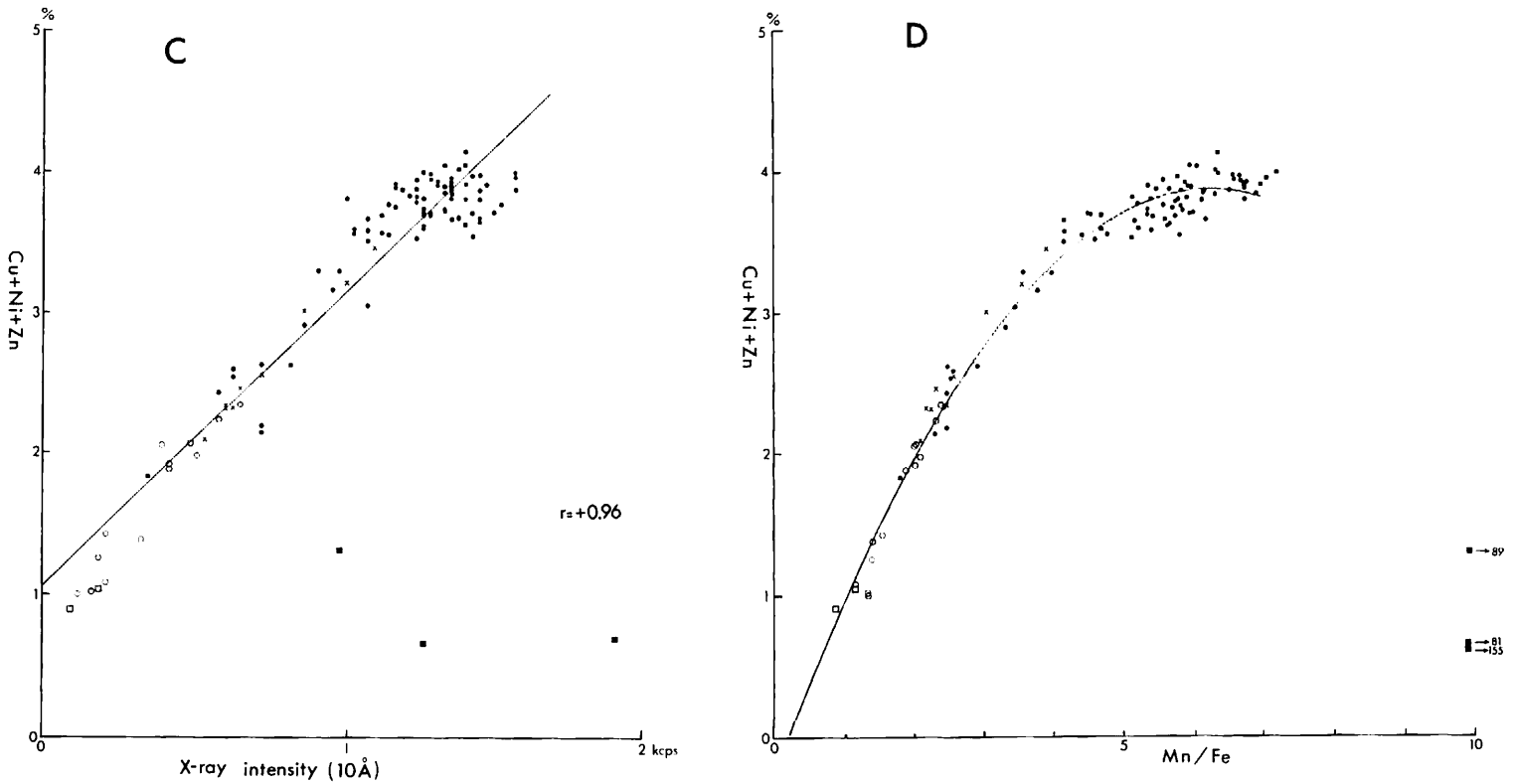
C
%
5
4
3
2
1
0
Cu+Ni+Zn
r=+0.96
0
1
2 kcps
X-ray intensity (10Å)
D
%
5
4
3
2
1
0
Cu+Ni+Zn
0
5
10
Mn / Fe
→89
→81
→155

Fig. XV-1(2)

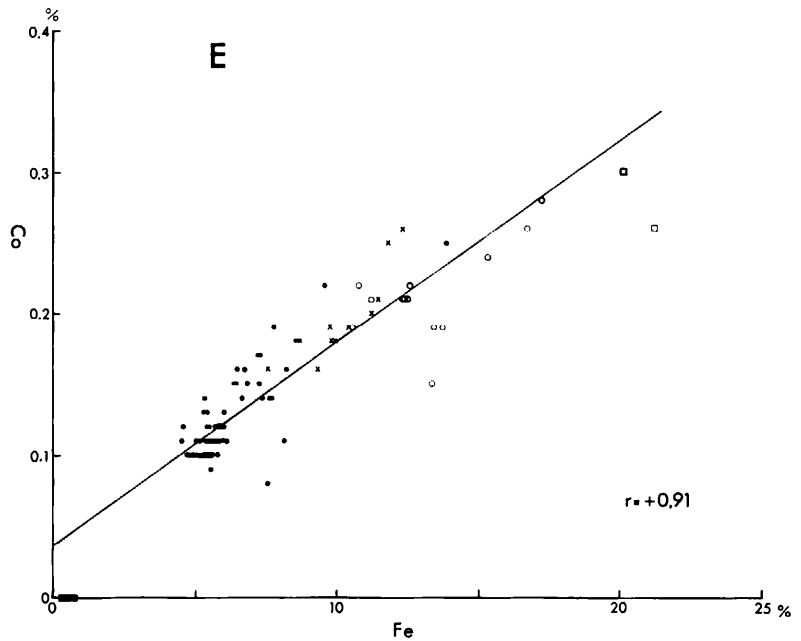

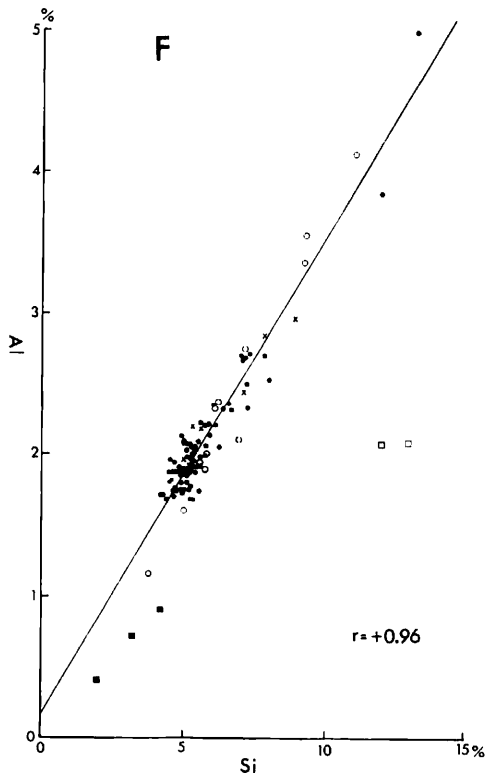

Fig. XV-1(3)

Table XV-3 Correlation matrix for chemical and mineral compositions of manganese nodules.

	Mn	Cu	Ni	Zn	Tl0	Qtz	Si	Al	Mmt	Ph	Pc	Fe	Co	Pb	H_2O^-	H_2O^+	D*
Mn	1																
Cu	0.92	1															
Ni	0.86	0.91	1														
Zn	0.92	0.93	0.86	1													
△Tl0	0.86	0.94	0.93	0.90	1												
△Qtz	0.47	0.52	0.72	0.49	0.59	1											
Si	−0.75	−0.54	−0.42	−0.56	−0.43	−0.04	1										
Al	−0.71	−0.49	−0.37	−0.53	−0.39	−0.04	0.96	1									
△Mmt	−0.60	−0.42	−0.33	−0.42	−0.31	−0.07	0.84	0.84	1								
△Ph	−0.58	−0.50	−0.50	−0.47	−0.45	−0.30	0.55	0.61	0.46	1							
△Pc	−0.24	−0.13	0.00	−0.14	0.00	0.23	0.42	0.44	0.34	0.20	1						
Fe	−0.81	−0.93	−0.95	−0.88	−0.95	−0.67	0.28	0.24	0.19	0.40	−0.04	1					
Co	−0.64	−0.77	−0.82	−0.78	−0.84	−0.59	0.06	0.03	−0.05	0.18	−0.15	0.91	1				
Pb	−0.68	−0.84	−0.81	−0.78	−0.83	−0.50	0.19	0.14	0.09	0.31	0.03	0.89	0.85	1			
H_2O^-	−0.49	−0.58	−0.70	−0.62	−0.65	−0.69	−0.01	−0.04	−0.10	0.22	−0.21	0.74	0.79	0.67	1		
H_2O^+	−0.30	−0.42	−0.47	−0.40	−0.46	−0.43	−0.14	−0.12	−0.08	0.15	−0.22	0.52	0.55	0.48	0.38	1	
△D*	−0.73	−0.83	−0.80	−0.79	−0.90	−0.52	0.31	0.26	0.17	0.34	0.05	0.85	0.78	0.75	0.60	0.39	1

Number of data sets: 103 (P218 and B63 excluded)

Components/Tl0: 10 Å manganate, Qtz: quartz, Mmt: montmorillonite, Ph: phillipsite, Pc: plagioclase, D: δ-MnO_2.

△: mineral composition, *: calculated on a simple assumption.

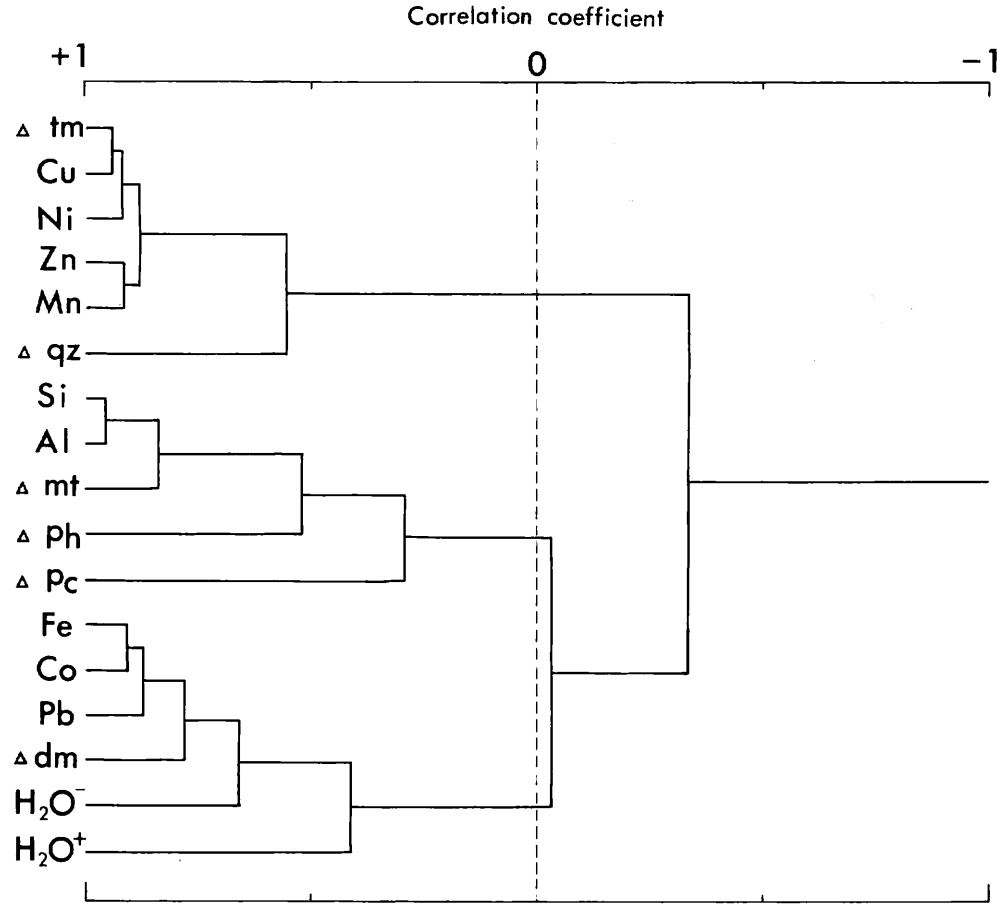

Fig. XV-2 Cluster analysis of chemical and mineral composition, showing three distinct groups. Analysis is based on correlation coefficients in Table XV-3. New coefficients between two components or groups are calculated by simple arithmetical averaging. Components/tm: 10 Å manganate, qz: quartz, mt: montmorillonite, ph: phillipsite, pc: plagioclase, dm: δ-MnO_2. Symbols with a small triangle denote mineral components.

with nodule mineralogy. Therefore nodule surface feature is closely related with bulk chemistry (MORITANI *et al.*, 1977; SOREM *et al.*, 1979) when their internal structure is simple Nodules of rough surface composed to 10 Å manganate are generally high in Mn, Cu, Ni, and Zn concentrations and ratio Mn/Fe, and low in Fe, Co, and Pb. Nodules of smooth surface composed of δ-MnO_2 are low in Mn, Cu, Ni, and Zn and ratio Mn/Fe, and high in Fe, Co, and Pb.

As shown in Table XV-2, nodule bulk compositions are markedly related to nodule morphological type, in accordance with relative abundance of the two manganese minerals and nodule surface feature. All parameters increase or decrease in the order of R2(Sr/Dr), I2(Ss.r/Ds.r), R1(IDr/IDPr), I1(IDs.r/IDPs.r), S1+S2(IDs/IDPs/Ds). The contrary order of R1 and I2 may be due to different mineral compositions between

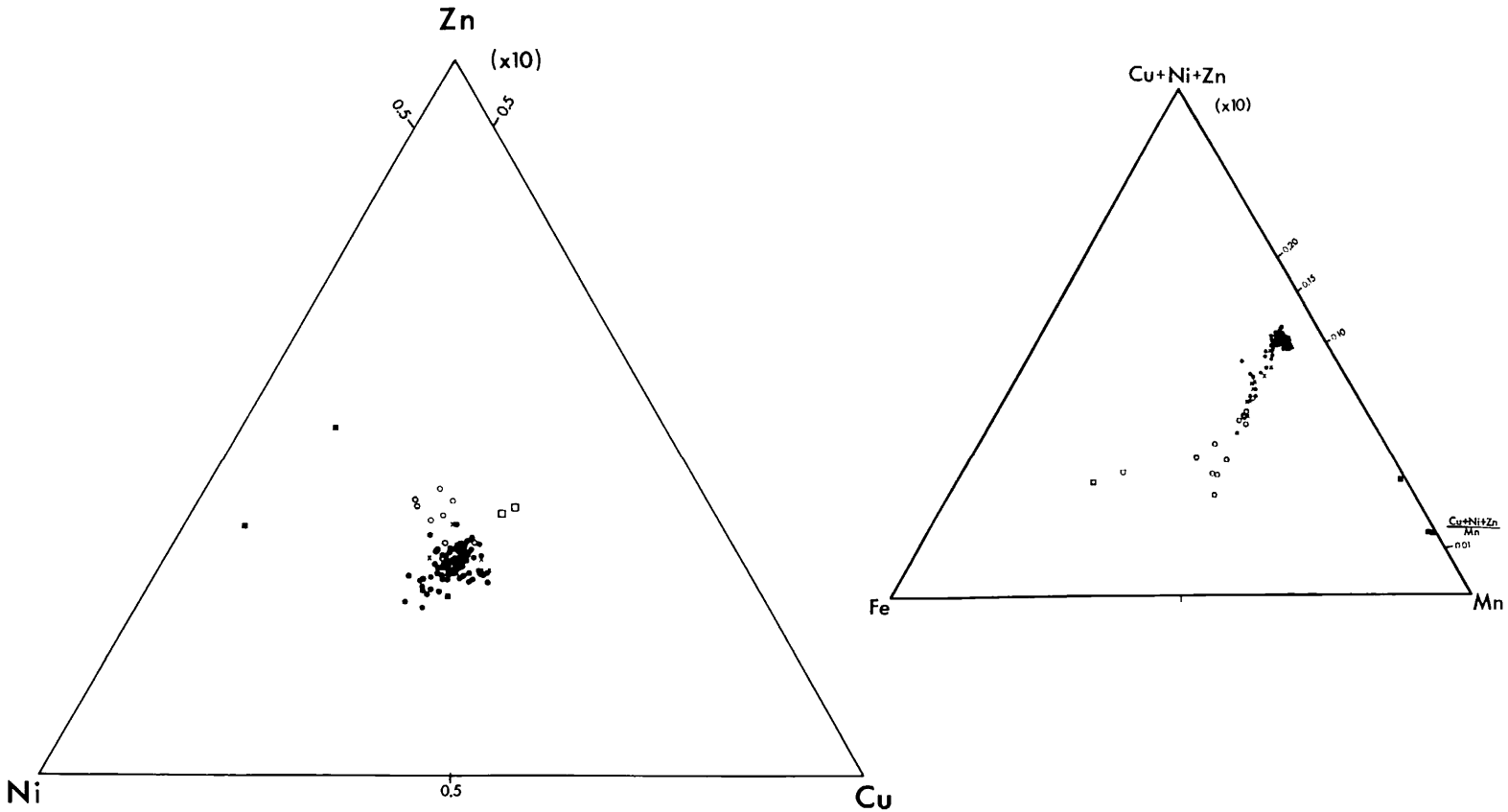

Fig. XV-3 Ternary diagrams showing ratios Fe/Mn/(Cu+Ni+Zn) and Cu/Ni/Zn. A) total Cu+Ni+Zn is dependent of Fe and Mn. Intersections of extrapolated line and triangle axes represent the compositions of 10 Å manganate and δ-MnO_2. B) Ratio Cu/Ni/Zn is considerably invariable except for buried nodules in B63 and P218. Symbols are common to Fig. XV-1.

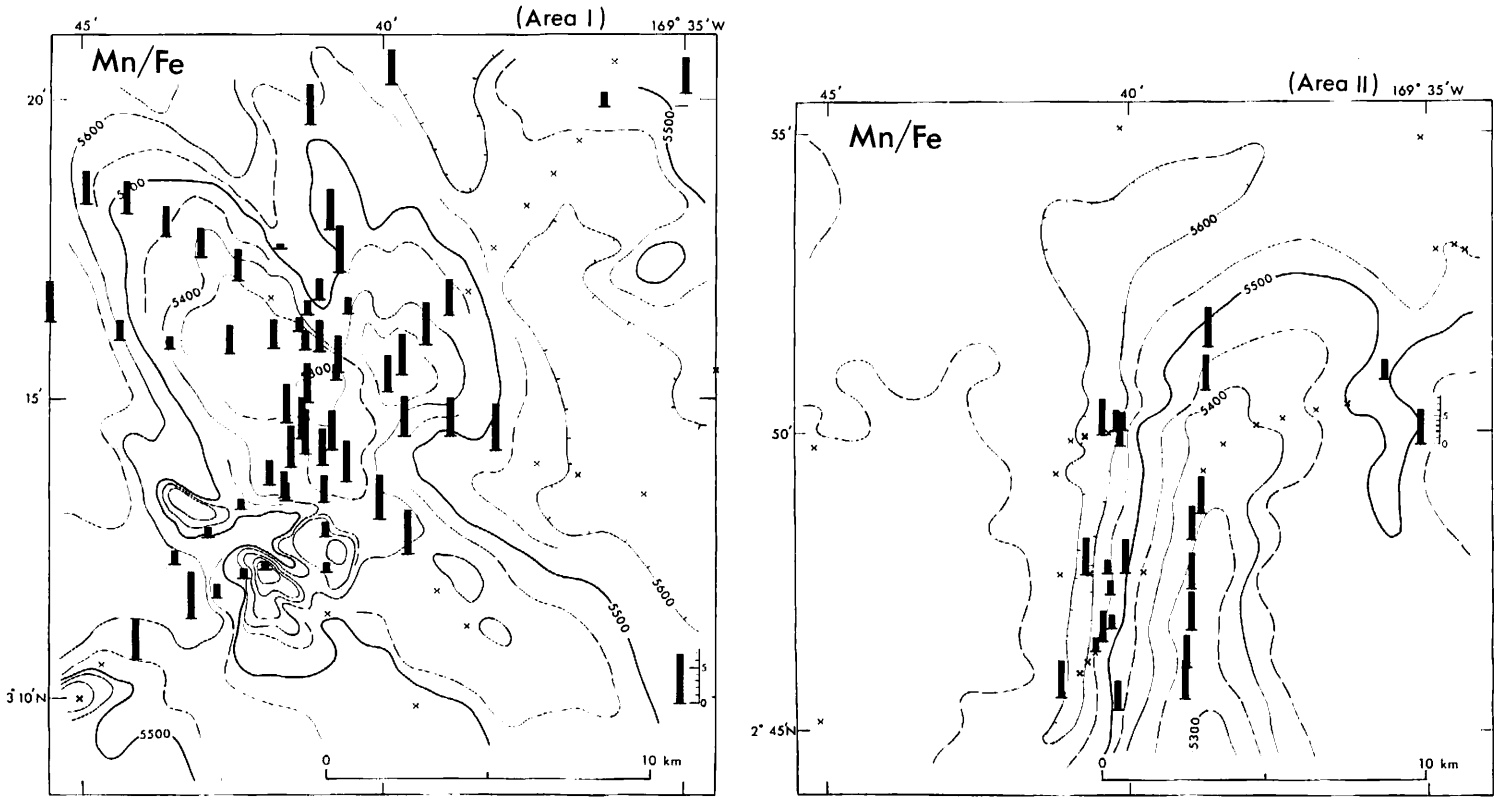

Fig. XV-4(1)

Fig. XV-4 Areal distribution of nodule chemical compositions in the detailed survey areas I and II. Three parameters consistently vary with nodule type. x: no nodule.

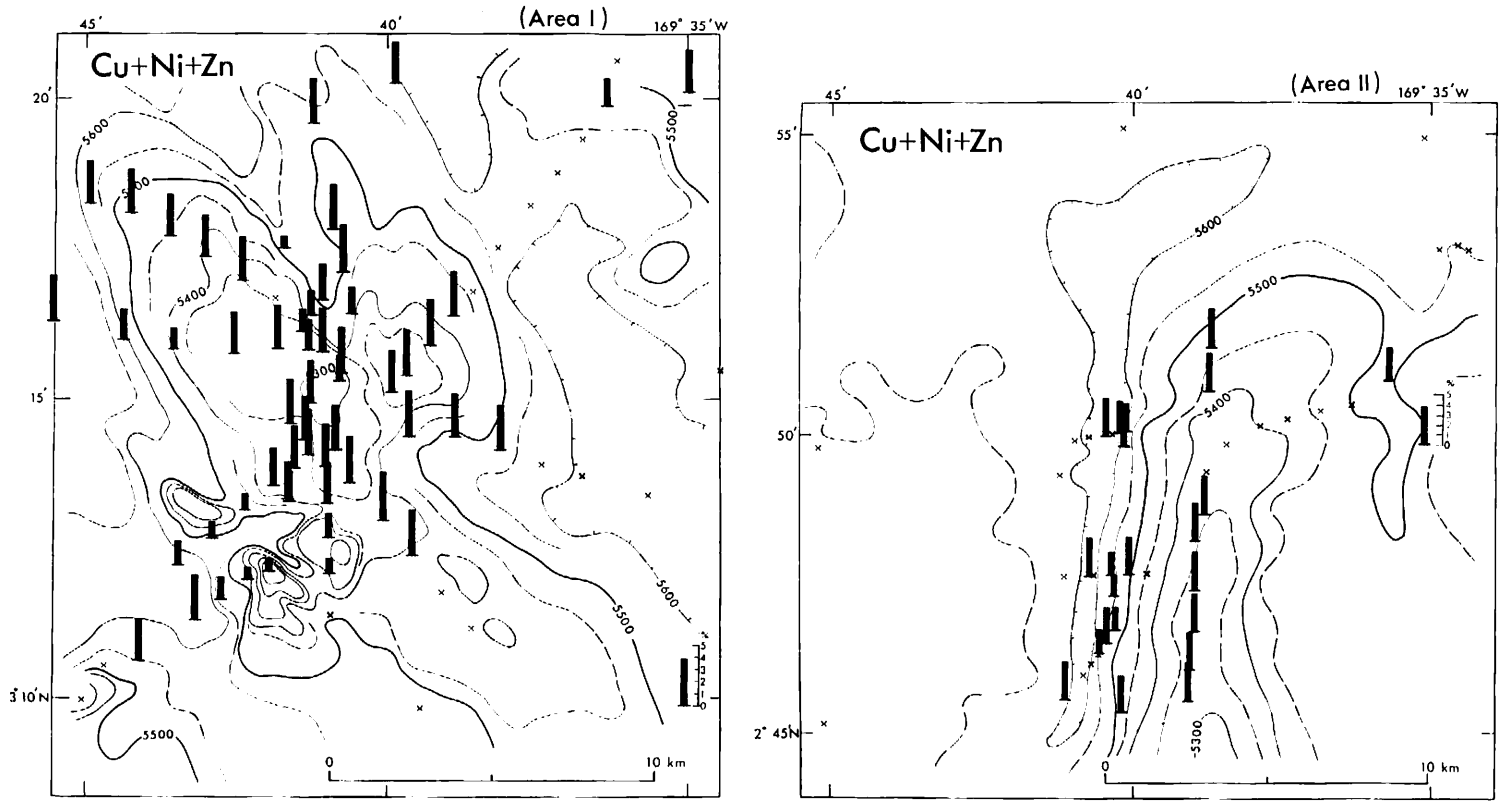
(Area I)
Cu+Ni+Zn
45′
40′
169° 35′W
20′
15′
3° 10′N
5600
5500
5400
5300
0
10 km
(Area II)
Cu+Ni+Zn
45′
40′
169° 35′W
55′
50′
2° 45′N
5600
5500
5400
5300
0
10 km

Fig. XV-4(2)

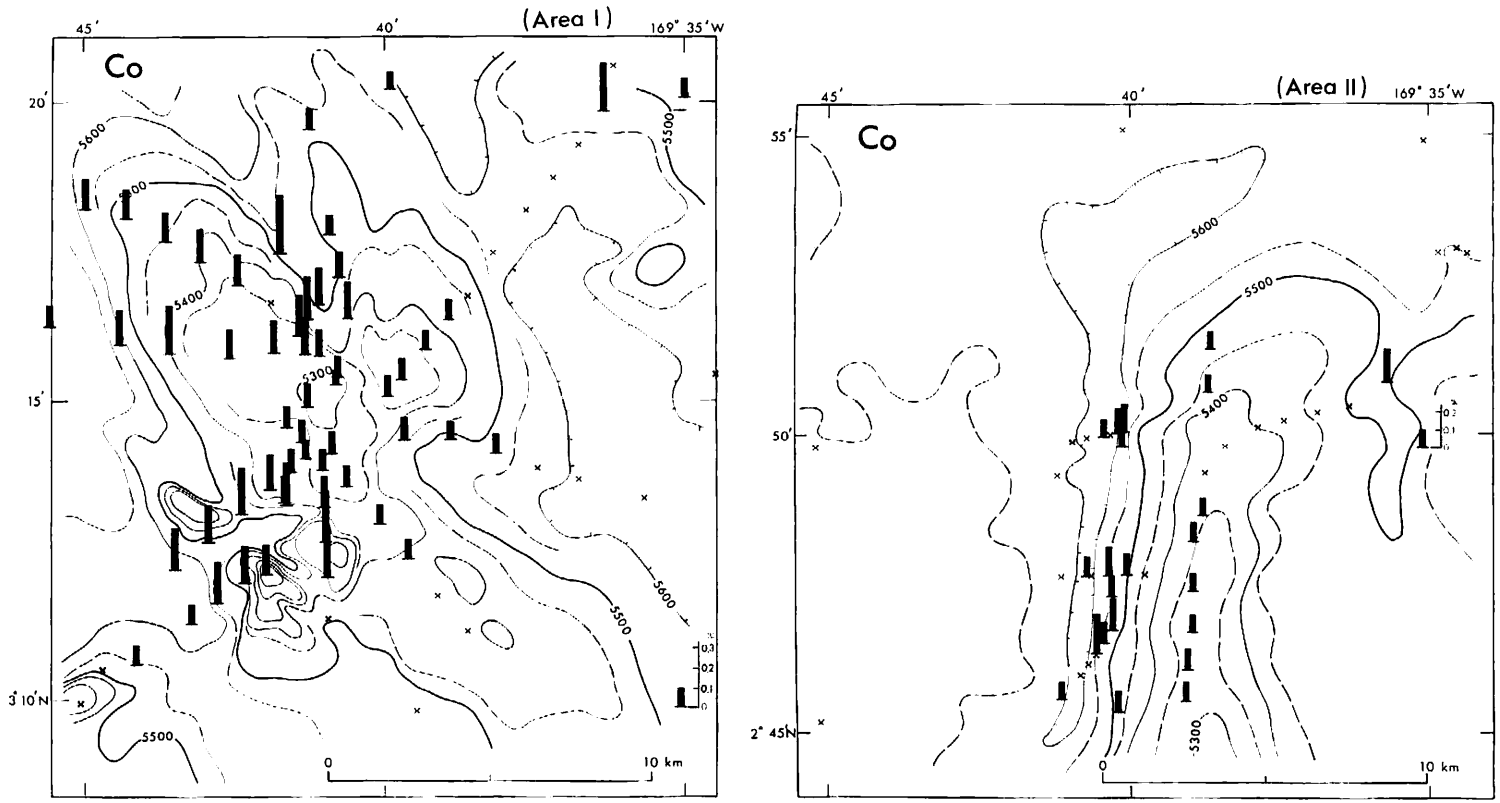
(Area I)
45′
40′
169° 35′W
Co
20′
15′
3° 10′N
5600
5500
5400
5300
0
10 km
(Area II)
55′
50′
2° 45′N
0.3
0.2
0.1
0

Fig. XV-4(3)

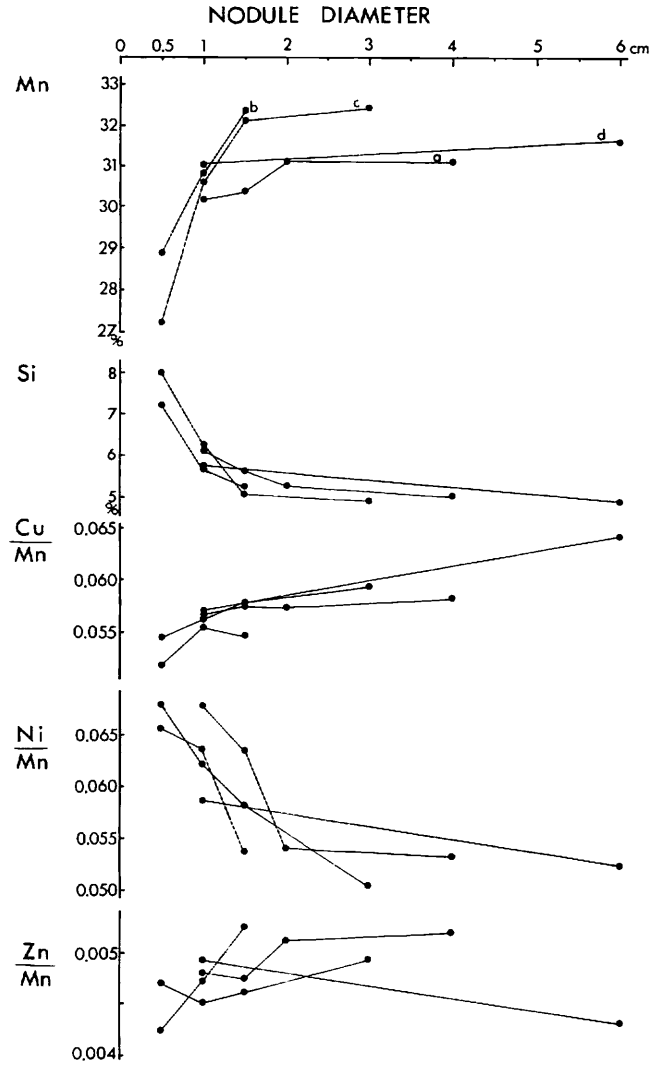

Fig. XV-5 Size-dependent compositional variations of r-type nodules. Stations/a: FG369, b: B65, c: FG424, d: D496.

nodule inside and outermost surfaces.

According to the above mentioned mineralogical characterization, following assumptions seem to be reasonable though it would be over-simplified one to explain every compositional features. 1) 10 Å manganate is a stoichiometric manganate with invariable ratio (Cu+Ni+Zn)/Mn, and contains no iron, 2) δ-MnO_2 contains no Cu, Ni, or Zn. Fe/Mn(=1.0) and Fe/Co are constant, 3) aluminosilicate fractions are variable but do not exceed 10 wt.% as SiO_2 and Al_2O_3. Inter-element correlations of bulk nodule samples (Fig. XV-1) are compatibly explained on these assumptions. Major elements, Mn and Fe, are weakly correlated and of scattered pattern due to

variable content of aluminosilicate fractions (Fig. XV-1A). The plots of Cu+Ni+Zn versus Mn shows a relatively dispersed pattern (correlation coefficient r= +0.91), and some fraction of total manganese is not related to Cu+Ni+Zn (Fig. XV-1B). However the plots of Cu+Ni+Zn versus 10 Å reflection intensity show strong linear dependency to 10 Å manganate abundance (r= +0.96), and the regression line may pass near the zero point (Fig. XV-1C).

On these assumptions Fe/Mn should be linearly dependent of relative abundance of δ-MnO_2 to the both minerals. Total Cu+Ni+Zn is therefore expected to vary as a hyperbolic function of the reciprocal, Mn/Fe. Fig. XV-1D well supports the assumptions. Concentration of Co mostly incorporated in δ-MnO_2 is positively correlated with Fe (Fig. XV-1E).

The cluster analysis (Fig. XV-2) based on correlation coefficient matrix (Table XV-3) reveals three significant component groups: 1) 10 Å manganate, Mn, Cu, Ni, Zn, and quartz, 2) δ-MnO_2, Fe, Co, Pb, and water contents, 3) Si, Al, and silicate minerals. These three groups are again consistent with the above mineral characterizations and assumptions.

In the ternary diagram (Fig. XV-3A), the total of Cu, Ni and Zn concentrations seems to be linearly dependent of Mn and Fe concentrations. The two intersections of the extrapolated regression lines and triangle axes are regarded as ideal compositions of 10 Å manganate and δ-MnO_2.

Typical areal distribution patterns of nodule chemistry are illustrated in Fig. XV-4. Mn/Fe ratio dependent of relative mineral composition generally agrees with nodule morphological type. The ratio is always low ranging from 1 to 2 for smooth surface nodules (type s) from the vicinity of southeastern sub-peaks in the Area I, intermediate surface nodules from the northern valleys in the Area I, and from the western flank of the Area II (see in Figs. VIII-7 and VIII-8). In contrast rough surface nodules (type r) always represent high Mn/Fe ratio and high Cu+Ni+Zn as a result of dominant development 10 Å manganate. Co concentrated in δ-MnO_2 is related to smooth to intermediate surface nodules throughout these areas.

Therefore the local variability of bulk nodule chemistry is primarily determined by abundance of manganese minerals. It is reasonable that these manganese minerals are considerably invariable in chemical composition irrespective of nodule abundance, size, or locality.

The ratio among Cu, Ni and Zn is generally invariable and irrespective of nodule type or locality (Fig. XV-3B). And this fact explains why Cu, Ni, Zn and Mn are positively correlated in bulk nodule compositions. However, in addition to those primary variation patterns in relation to mineral abundance, secondary smaller variations are observed. A size-dependent compositional variation was observed in some stations as shown in Fig. XV-5. These stations yield abundant spherical nodules of type r (Sr) whose diameter ranges from several centimeters to less than 5 millimeters.

Inverse pattern of variations between Mn and Si may be due to relatively great abundance of silicate minerals in smaller nodules. Fig. XV-5 markedly shows that Ni is relatively enriched in smaller nodules (than ca. 1 cm) as compared with Cu and Zn although the range of variation is not very great. This fact cannot be explained only by mineral abundance in manganese nodules, suggesting a minor compositional variabil-

ity of the manganese mineral. It may be attributable to preferential accumulation of Ni into 10 Å manganate lattice in the initial growth stage of nodules, or to active metal supply source rich in Ni. We have no further data now to give a conclusive explanation to this fact.

Plots of Si versus Al show a strong positive correlation with linear regression line crossing near the zero point (Fig. XV-1F). The mean atomic ratio Si/Al of the nodules is around 2.6 ranging from 2.2 to 3.2. It is consistent with reported value for marine phillipsites (2.4 to 2.8: BOLES, 1977). It may be suggested that phillipsite is the most dominant aluminosilicate fraction of these nodules.

Chemical composition of buried manganese concretions

Buried manganese concretions from this area, especially from the piston core P218, have extraordinary chemical compositions. The irregular concretions from P218 at a depth of 32 cm are composed of a strikingly pure manganate mineral containing traceable amounts of Fe, Cu, Ni, Zn, Co, and Pb. The mineral components are well crystalline 7 Å manganate (or birnessite) which is very rarely found in deep-sea nodules and 10 Å manganate (USUI, this cruise report). This anomalous mineral and chemical compositions suggest a different environement of formation from normal deep-sea manganese nodules; for instance hydro thermal.

Nodules from the box core B83 at a depth below the sea-bottom of 15 cm is of typical smooth surfaces partly covered with dense clayey material. The chemical composition is around the range of s-type nodules but much enriched in Fe and depleted in Mn, Cu, Ni and Zn.

Summary

Manganese nodules of high concentration of Cu, Ni, and Zn, comparable to the Northeastern Equatorial Manganese Nodule Belt are, locally distributed in this area, though compositional variation is considerably great. The small-scale sampling of manganese nodules and comparative chemical and mineralogical analyses reveal that the local variation of nodule chemistry of the GH81-4 area is principally due to preferential development of 10 Å manganate and δ-MnO_2. General compositional characteristics and inter-element correlations are reasonably explained in terms of the mineral characterization of the two minerals and aluminosilicate minerals.

The local variability of nodule morphological type is generally consistent with bulk chemical and mineral compositions. Rough surface nodules are enriched in Mn, Cu, Ni, and Zn, and depleted in Fe, Co, and Pb, reflecting the chemical composition of 10 Å manganate; and smooth surface nodules vice versa. The scheme is, however, not always applicable when the inside mineral composition is different from that of nodule surface.

In addition to these primary variation pattern, secondary variation dependent of diameter was found in 10 Å manganate nodules in some stations. Smaller nodules are enriched in Ni as compared with Cu and Zn. It suggests a possibility of minor compositional variability of 10 Å manganate.

Manganese concretions of irregular shape, anomalous chemical composition (Mn/Fe ratio; up to 155), and exceptional mineral composition was found from piston core

P218 at a depth of 32 cm. This characteristics suggest a different condition of formation normal deep-sea manganese nodules.

References

BOLES, J. R. (1977) Zeolites in deep-sea sediments. *In* F. A. MUMPTON (ed.) *Mineralogy and Geology of Natural Zeolites*. Mineral. Soc. Am. Short Course Notes, vol. 4, p. 137–163.

CRONAN, D. S. (1980) *Under Water Minerals*, Academic Press, Longon, pp. 362.

HALBACH, P. and ÖZKARA, M. (1979) Morphological and geochemical classification of deep-sea ferromanganese nodules and its genetical interpretation. *In* C. LALOU (ed.) *La Genèse des Nodules de Manganèse*. C. N. R. S. Rept. no. 289, p. 77–88.

HEIN, P. (1977) Geochemie des nodules du Pacifique nord-est: etude statistique. *Scientific and Technical Rept. CNEXO*, no. 35, p. 1–74.

MOCHIZUKI, T. and TERASHIMA, S. (1983) Chemical analysis of manganese nodules. Methods of Chemical Analysis in Geological Survey of Japan (in Japanese), no 53, pp. 36.

MORITANI, T., MARUYAMA, S., NOHARA, M., MATSUMOTO, K., OGITSU, T. and MORIWAKI, H. (1977) Description, classification, and distribution of manganese nodules. *Geol. Surv. Japan Cruise Report*, no. 8, p. 136–158.

PIPER, D. Z. and LEONG, K. (1979) Manganese nodule and surface sediment composition, Domes sites A, B, and C. *In* BISCHOFF, J. L. and PIPER, D. Z. (eds.), *Marine Geology and Oceanography of the Pacific Manganese Nodule Province*, Plenum Publ. Co., p. 437–473.

SOREM, R. K., REINHART, R. H., FEWKS, R. H. and MCFARLAND W. D. (1979) Occurrence and character of manganese nodules in Domes sites A, B, and C, East Equatorial Pacific Ocean. *In* BISCHOFF, J. L. and PIPER, D. Z. (eds.), *Marine Geology and Oceanography of the Pacific Manganese Nodule Province*, Plenum Publ. Co., p. 475–527.

TERASHIMA, S. (1978) Atomic absorption analysis of Mn, Fe, Cu, Ni, Co, Pb, Zn, Si, Al, Ca, Mg, Na, K, Ti and Sr in manganese nodules (in Japanese with Engligh abstract). *Bull. Geol. Surv. Japan*, vol. 29, p. 401–411.

USUI, A. (1979) Minerals, metal contents and mechanism of formation of manganese nodules from the Central Pacific Basin (GH76–7 and GH77–1 areas). *In*: BISCHOFF, J. L. and PIPER, D. Z. (Eds.), *Marine Geology and Oceanography of the Pacific Manganese Nodule Province*, Plenum, New York, pp. 651–677.

———, SHOJI, T. and TAKENOUCHI, S. (1978) Mineralogy of deep sea manganese nodules and synthesis of manganese oxides: Implications to genesis and geochemistry (in Japanese with English abstract). *Mining Geology*, vol. 28, p. 405–420.